Hybrid forms of beat phenomena in nuclear forward scattering of synchrotron radiation

Yu.V. Shvyd'ko [a] and U. van Bürck [b]

[a] *II. Institut für Experimentalphysik, Universität Hamburg, D-22761 Hamburg, Germany*
E-mail: yuri.shvydko@desy.de
[b] *Physik-Department E15, Technische Universität München, D-85748 Garching, Germany*
E-mail: uwe.vbuerck@ph.tum.de

In nuclear forward scattering (NFS) of synchrotron radiation, inter-resonance interference leads to a quantum beat (QB), and intra-resonance interference to a dynamical beat (DB). In general both interference processes determine the time evolution of NFS. Only in the case of far distant resonances the resulting interference pattern can be interpreted as a well distinguishable combination of QB and DB. Multiple scattering by near neighbouring resonances, by contrast, leads to a hybridisation of QB and DB. In particular, asymmetrical continuous distributions of resonances make QB and DB blend into a fast hybrid beat with thickness dependent period and distribution sensitive modulation.

1. Introduction

The development of intense pulsed sources of synchrotron radiation (SR) made the observation of pure nuclear Bragg scattering of SR [1] possible, providing the basis for Mössbauer spectroscopy in the time domain (for a review see, e.g., [2,3]). But only the introduction of meV-resolution X-ray monochromators made the observation of nuclear forward scattering (NFS) of SR feasible [4] and has thus opened a broad field of applications for time-domain spectroscopy.

In conventional Mössbauer spectroscopy the dependence of nuclear absorption on the energy of the incident radiation is measured. The recorded signal in this case presents the incoherent sum of the spectral components of the transmitted radiation. In time-domain spectroscopy, by contrast, the *scattering* spectrum of nuclei excited by a pulse of white SR is measured in the time domain, where the response is the *coherent* sum of the spectral components of the scattered radiation. This results in important interference effects specific for time-domain Mössbauer spectroscopy.

Interference of radiation scattered by nuclear resonances at different energies, arising, e.g., due to hyperfine interactions, leads to a quantum beat (QB) [5,6]. Henceforth we shall refer to interference of this type as inter-resonance interference. Multiple nuclear scattering within one resonance yields a dynamical beat (DB) in the time response of NFS [7–10]. Multiple resonance scattering via different resonances, by

contrast, i.e., the coherent combination of the two basic beat phenomena, results in general in hybrid forms of the beat.

Different hybrid forms of beat phenomena are the subject of this paper. Simple combinations of QB and DB, where the two kinds of beat can still be distinguished, and thus can be considered as independent, will be presented in section 2. The interference in case of discrete near neighbouring resonances, which leads to a hybridisation of QB and DB, will be discussed in section 3.1, and in section 3.2 the effect of a continuous distribution of resonances will be considered, which results, in the case of strongly asymmetric distributions, in a fast hybrid beat.

2. Quantum beat and dynamical beat

NFS of SR is, generally speaking, a complex coherent multiple scattering process. Mathematically this is expressed by a series of coherent multiple scattering amplitudes involving different resonances [11,12]. Each single scattering process is described by a double-time correlation function $K(t,\tilde{t})$ of the nuclear ensemble, giving a single scattering coherent response of the nuclear system at time t to an excitation at time $\tilde{t}$.

In our discussion of beat phenomena occurring in NFS we will proceed from simple to complex scattering processes: single scattering via several resonances – section 2.1, multiple scattering via a single resonance – section 2.2, and finally multiple scattering via several resonances – section 3.

2.1. Quantum beat

In the single scattering approximation, the radiation amplitude $A(t)$ at time t after an instantaneous excitation of a nuclear ensemble at time $t = 0$ is proportional to the double-time correlation function $K(t,0)$ [11]. For time-independent hyperfine interactions it can be presented as

$$A(t) \propto -K(t,0) = -\xi \sum_{\ell} a_\ell \exp\left(-\frac{\mathrm{i}}{\hbar} E_\ell t - \frac{t}{2\tau_0}\right). \tag{2.1}$$

Here τ_0 is the nuclear lifetime, $\xi = \sigma_0 N d f_{\mathrm{LM}}/4$ is the effective thickness parameter of the sample, with σ_0 the nuclear resonance cross section, N the density of resonant nuclei, d the sample thickness, and f_{LM} the Lamb–Mössbauer factor. The values a_ℓ ($|a_\ell| \leqslant 1$) represent the relative scattering amplitudes of different resonances ℓ with energies E_ℓ.

The observable time spectrum, which is given by $I(t) \propto |A(t)|^2$, contains a sum of sinusoidal functions, producing periodic modulations of the signal with difference frequencies $(E_{\ell'} - E_{\ell''})/\hbar$. These modulations have been named quantum beats (QB) [5,6]. Usually the different resonances originate from hyperfine interactions in one and the same sample. They can, however, also be experimentally produced by a Doppler shift between different samples moving at constant velocity. Examples of

simple QBs with a single beat frequency resulting either from the two $M - m = 0$ hyperfine transitions in ^{57}Fe metal or from a Doppler shift between two targets of stainless steel $^{57}Fe_{55}Cr_{25}Ni_{20}$ (SS) can be found in [12, figure 3] and in figure 3(A) of this paper, respectively.

2.2. Dynamical beat

Multiple nuclear scattering already within each resonance leads to another type of modulation of the amplitude of the forward scattered radiation. In the case of a single resonance this modulation is given by [8]

$$A(t) \propto -\xi \exp\left(-\frac{\mathrm{i}}{\hbar}E_0 t - \frac{t}{2\tau_0}\right)\frac{J_1(2\sqrt{\xi\tau})}{\sqrt{\xi\tau}}, \tag{2.2}$$

where E_0 is the nuclear resonance energy and J_1 is the Bessel function of first kind and first order, and $\tau = t/\tau_0$. The resulting modulation of the NFS intensity is called dynamical beat (DB).

The DB exhibits characteristic features which are quite general for the propagation of electromagnetic radiation pulses through a resonant medium, which will be of importance for the later discussion:

1. The DB is aperiodic, the apparent periods increase with time.
2. The apparent DB periods decrease with increasing thickness ξ.
3. The initial decay is sped up proportionally to thickness ξ.
4. The field amplitude $A(t)$ changes sign at every beat.

These features are obvious from the above expression for $A(t)$. A detailed discussion and explanation can be found in [13]. Examples of DBs for single-resonance targets of different thicknesses of SS and $(NH_4)_2Mg^{57}Fe(CN)_6$ are given in [13, figures 2 and 3, respectively].

A simplified but useful explanation of the DB can be obtained [3] by considering the energy spectrum of the NFS intensity $|A(E)|^2$, where $A(E) = 1 - R(E)$ with $R(E)$ the transmission amplitude as, e.g., given in [12]. Such a spectrum is displayed in figure 1a for a single-resonance material. The spectrum exhibits a double-hump structure which is typical for optically thick samples, and which arises from enhanced scattering and diminished absorption on the wings of the resonance. In this picture, the DB results from the interference of the dominant contributions above and below resonance. These contributions, with separation $\simeq \hbar\omega_{\mathrm{D}}$, lead to a DB with frequency of order ω_{D} which is also displayed in figure 1a.

2.3. Distinguishable combinations of quantum beat and dynamical beat

In the case of several resonances multiple resonance scattering occurs, generally speaking, not only via one and the same resonance, but also via different resonances.

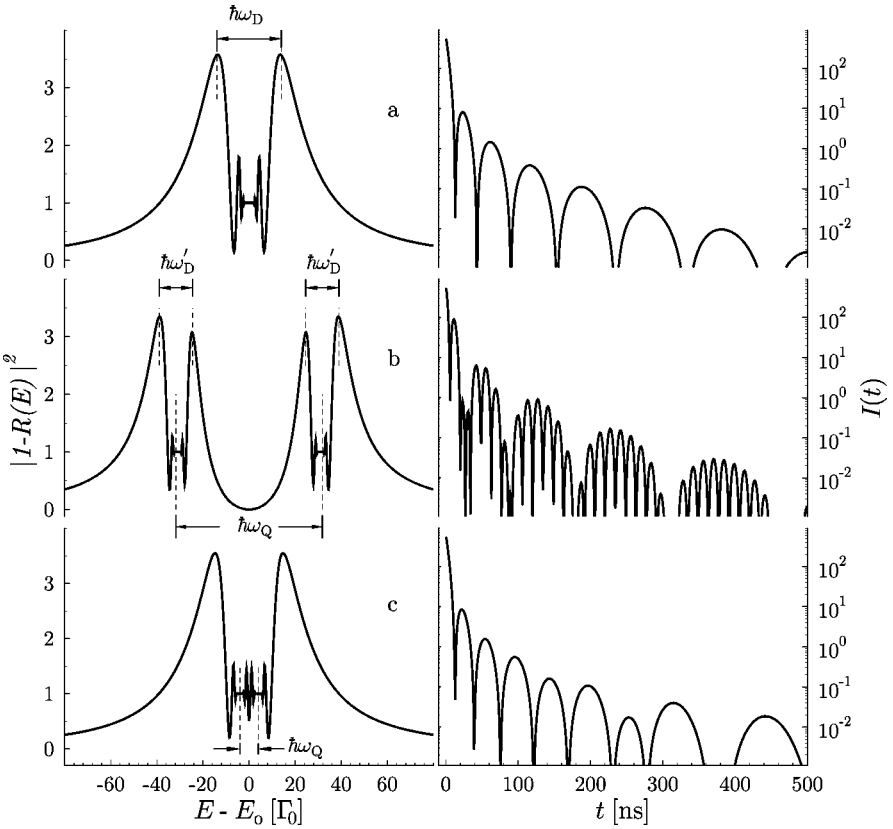

Figure 1. Energy and time dependences of the NFS intensity in case of an optically thick scatterer ($\xi = 41.3$) with one resonance (a) and two resonances separated by a large ($\hbar\omega_Q = 63\Gamma_0$) (b) or a small ($\hbar\omega_Q = 8\Gamma_0$) (c) hyperfine splitting, with Γ_0 the natural linewidth. Each resonance shows the typical double-hump structure, with separation of the two humps by $\hbar\omega_D$ (in a) and $\hbar\omega'_D$ (in b). Note that $\omega'_D \simeq \omega_D/2$. The situation (a) yields a DB with apparent frequency of order ω_D. The situation (b) gives a time evolution characterised by a fast QB with frequency ω_Q, modulated by a DB with a frequency of order ω'_D. The situation (c) leads to a so-called slow hybrid beat.

This results in a more complicated time response of the nuclear system where QB and DB melt together. However, in some cases one can still think in terms of an independent combination of QB and DB. This happens if the energy separation of the resonances $E_{\ell'} - E_{\ell''}$ is large in comparison with the extension of the double-hump structures of the resonances ℓ participating in the scattering and if the observation time t is not too long. Such cases are considered in this section in order to give a contrast to the hybrid forms of beat phenomena discussed below.

In case of far separated resonances one can neglect multiple scattering paths via different resonances and make the approximation (see, e.g., [9,12]) that the time evolution of the amplitudes $A_\ell(t)$ of the radiation components of resonance ℓ are approximately given by eq. (2.2), where for each resonance the appropriate effective

thickness parameter $\xi_\ell = a_\ell \xi$ is used. The resulting field will then be given by the sum of all contributions:

$$A(t) \propto \sum_\ell A_\ell(t) = -\sum_\ell \xi_\ell \exp\left(-\frac{\mathrm{i}}{\hbar} E_\ell t - \frac{t}{2\tau_0}\right) \frac{J_1(2\sqrt{\xi_\ell \tau})}{\sqrt{\xi_\ell \tau}}. \tag{2.3}$$

2.3.1. Two equivalent resonances

In case of two resonances with equal effective thickness $\xi_\ell = \tilde{\xi}$ this approximation leads to a DB-modulated QB time spectrum:

$$I(t) \propto 4\tilde{\xi}^2 \cos^2\left(\frac{\omega_\mathrm{Q} t}{2}\right) \exp\left(-\frac{t}{\tau_0}\right) \frac{J_1^2\left(2\sqrt{\tilde{\xi}\tau}\right)}{\tilde{\xi}\tau}, \tag{2.4}$$

where $\hbar\omega_\mathrm{Q}$ is the energy separation between the two resonances. Examples of such DB-modulated QBs can be found in [14, figure 6] or in [13, figure 1] for NFS of SR by the $M - m$ = 0 hyperfine transitions of ^{57}Fe metal foils of $\sim$5 and 9 μm thickness, respectively. A typical NFS energy spectrum calculated for the case of two well separated hyperfine transitions of equal strengths is depicted in figure 1b together with the corresponding time spectrum, which clearly exhibits the DB-modulation of the QB.

In reality, however, there always remains a weak influence of multiple scattering via different resonances. This influence leads, for instance, to a slight shift of the QB pattern in time, proportional to sample thickness [10]. Such a shift of the QB had been revealed first in Bragg scattering by comparing different time evolutions observed in Laue and in Bragg geometry [15]. In the case of two resonances, such a shift can be simply understood as due to an increase (decrease) of the refractive index at the lower-energy (higher-energy) resonance by the influence of the higher-energy (lower-energy) transition, respectively. The effect of this asymmetric change of the refractive index at the two transitions can be accounted for in first approximation by an additional phase in the argument of the $\cos^2$-factor in eq. (2.4). In the double-hump picture of figure 1b the effect of the inter-resonance interference on the intra-resonance interference is noticed by the slight asymmetry of each double-hump.

2.3.2. Non-equivalent resonances

In the case of non-equivalent resonances which exhibit different thickness parameters ξ_ℓ, the dynamical evolution of the forward scattered radiation amplitudes $A_\ell(t)$ will be different for each resonance ℓ. In the single-resonance approximation of eq. (2.3) this leads to a time-dependent interference contrast.

The simplest case of two non-equivalent resonances can be experimentally obtained by mounting two single-resonance targets of different optical thickness downstream behind each other, keeping one at rest and moving the other at constant Doppler velocity. The result of such a measurement performed with SS foils [16] can be found in [13, figure 5], where the time dependence of the interference contrast and phase

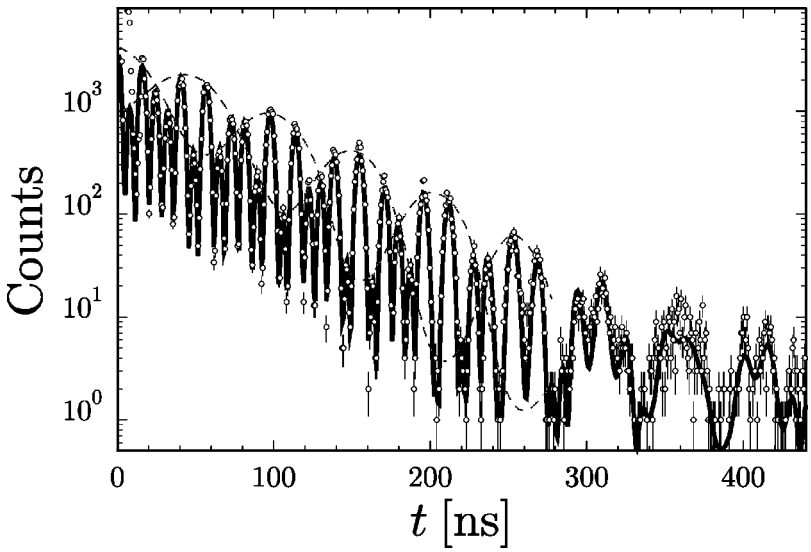

Figure 2. Time evolution of NFS of SR for a 1 μm iron metal foil in a horizontal magnetic field of ∼0.13 T. The solid lines are fits using the NFS theory [11]. The dashed lines are guidelines to the eye, pointing out a ∼100 ns modulation of the fast beat, starting high (low) at time zero for the even (uneven) numbered beats, respectively.

jumps of the QB connected with sign changes of the amplitude $A(t)$ of the thicker foil are well recognized.

The amplitude modulation of the QB becomes more dramatic when more than two resonances are involved in the inter-resonance interference. A well known example is that of the four $M - m = \pm 1$ hyperfine transitions in ^{57}Fe, with ratios 3 : 1 : 1 : 3 of the scattering amplitudes and resulting effective thicknesses ξ_ℓ. The time evolution of NFS in this case [12] is depicted in figure 2. At very early times the scattering is dominated by the strong contributions of the outer resonances, the interference of which gives rise to a fast QB with ∼8 ns period. At later times, however, the dynamical modulation makes these radiation components temporarily disappear. As a result, at times $t \sim 360$ ns only the scattering of the inner resonances is observed, which is characterized by a slow QB of ∼50 ns period. A more detailed analysis of the QB in this case can be found in [12].

The interesting case of three equidistant resonances with ratios 1 : 2 : 1 of the effective thickness can be modelled by means of Doppler shifts. It is observed in backreflection geometry [17], when two identical SS targets are mounted behind each other, with one kept at rest and the other being moved at constant velocity. Figure 3b displays the result of this experiment [18]. Initially the inter-resonance interference leads to a QB $\sim \cos^4(\omega_{\rm Q} t/4)$ as predicted by single scattering for such a distribution of oscillators, where $\hbar\omega_{\rm Q}$ is the separation of the two outer resonances. Due to the dynamical modulation, however, the radiation field of the stronger central resonance decreases faster than the fields of the outer resonance components. Its amplitude goes

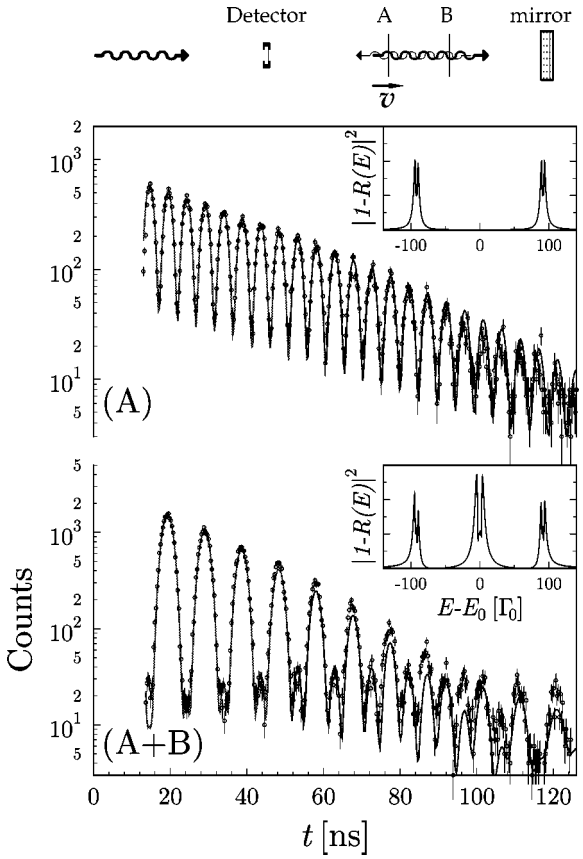

Figure 3. Time evolution of NFS of SR in backreflection geometry: (A) a single SS target of ∼1.3 μm thickness moved at constant velocity v, corresponding to a Doppler shift of $91.7\Gamma_0$; (A + B) two identical SS targets, A moving with v and B at rest. The corresponding weights of resonances are 1 : 0 : 1 (A) and 1 : 2 : 1 (A + B). The solid lines are fits using the NFS theory [11]. The insets show the corresponding energy spectra of NFS.

through zero at times $t \sim 95$ ns. Then the contributions of the outer two resonances are left alone, the interference of which gives a QB $\sim \cos^2(\omega_Q t/2)$ with double frequency, comparable to the one obtained in total absence of the foil at rest, which is depicted in figure 3a. Later on, the radiation field of the central resonance recovers, however with negative amplitude, and the QB develops to $\sim \sin^4(\omega_Q t/4)$.

3. Hybrid beat

The examples of the previous sections demonstrate that in NFS of SR the multiple scattering of the radiation within each resonance strongly changes the appearance of the QB pattern in time. To some extent, these patterns already represent hybrid forms of beating. However, these beat patterns can still be "read" and understood in the

single-resonance approximation of eq. (2.3). Such an analysis of the time evolution of NFS is usually possible when the separation of the resonances is large in comparison with the extensions of the double-hump structures. This is equivalent to the DB being slow in comparison with the QB.

In the opposite case, however, when the resonances are close to each other and when the DB is fast in comparison with the QB, combined inter- and intra-resonance interference leads to results which can no longer be interpreted in the picture of well distinguishable QB and DB. In this case we have also to consider effects of multiple scattering via different resonances.

3.1. Slow hybrid beat

The situation with two closely lying resonances is depicted in figure 1c. It is obvious that in case of a relatively small separation of the resonances, the result of the interlacing radiation field amplitudes will by no means be a modulation of the DB by a slow QB, but rather a hybridised form of QB and DB. The result of this complicated interference in the time domain is uncertain. One could, for instance, expect that the modified DB will be faster than for an unsplit resonance, because the two humps become more separated by the resonance splitting in combination with destructive interference between the lines. Or one could expect that it will be slower because the scattering strength and thus the effective thickness in each resonance is reduced by the splitting.

This type of hybridisation, which we shall refer to as slow hybrid beats, was recently studied in an experiment [19]. Again two identical targets of a single-resonance material were placed downstream behind each other, one being moved at different constant velocities. With respect to NFS, this sample combination is equivalent to a target with variable two-line splitting.

In figure 4 the time evolution of NFS of SR for two SS foils of $\sim$1.3 μm thickness each is shown for increasing Doppler shifts ΔE. The limiting cases are $\Delta E = 0$ (figure 4a), where a pure DB corresponding to 2.6 μm thickness (first DB minimum at $\sim$100 ns) is observed, and $\Delta E = \pm 180\Gamma_0$ (figure 4d), where a QB of about 5 ns period is modulated by a DB corresponding to 1.3 μm thickness (first DB minimum outside the observation window at $\sim$200 ns). In the first case the nuclear excitations of both samples are strongly coupled via their radiation field, whereas in the latter case radiative coupling takes place only within each of the samples. The point of interest is the transition from one case to the other. Already when a small Doppler shift of $\sim 2\Gamma_0$ is introduced (figure 4b), the DB minimum is shifted to $\sim$92 ns. This shift to earlier times goes on continuously for increasing Doppler shifts (figure 4c). Thus in spite of the reduction of the effective thickness parameter ξ in each resonance connected with the resonance splitting, the first minimum of the DB was immediately shifted to earlier times, corresponding to a larger separation of the two humps in the double-hump picture.

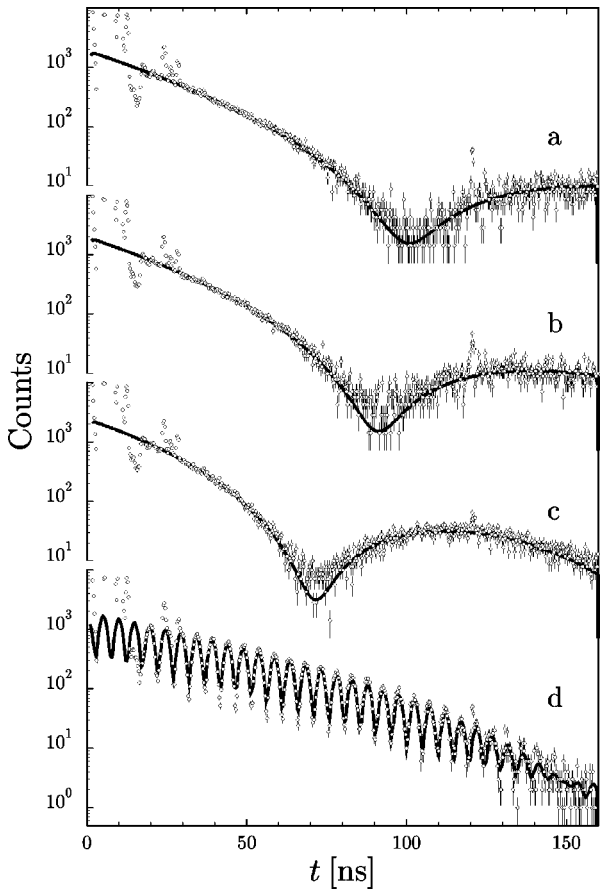

Figure 4. Time evolution of NFS of SR from two ∼1.3 μm SS foils, where one foil was moved at constant velocities corresponding to Doppler shifts of 0 (a), 2 (b), 4 (c) and $180\Gamma_0$ (d). The solid lines are fits using the NFS theory [11].

In order to study this hybridisation also in the case of a faster DB, the experiment was repeated for SS foils of ∼7 μm thickness each. The result is shown in figure 5. In the case $\Delta E = 0$ (figure 5a) a pure DB corresponding to 14 μm thickness is observed (DB minima at ∼20, 67 and 140 ns), and in the case $\Delta E = \pm 180\Gamma_0$ (figure 5d) a QB of about 5 ns period is modulated by a DB corresponding to 7 μm thickness (DB minima at ∼40 and 134 ns). In the transition region between these two cases QBs arise, the period of which is more and more reduced with increasing Doppler velocity. During the transition, DB and QB melt together, and can no longer be identified separately. In this process, neighbouring beat minima may for instance converge, making the beat maximum between them vanish completely, as, e.g., observed for the third maximum at ∼50 ns, which disappears when ΔE is increased from ∼16 to $24\Gamma_0$ (compare figure 5b). For large Doppler velocities, by contrast, the samples are radiatively almost decoupled, and the DB modulation stays constant, being determined by each sample alone. This

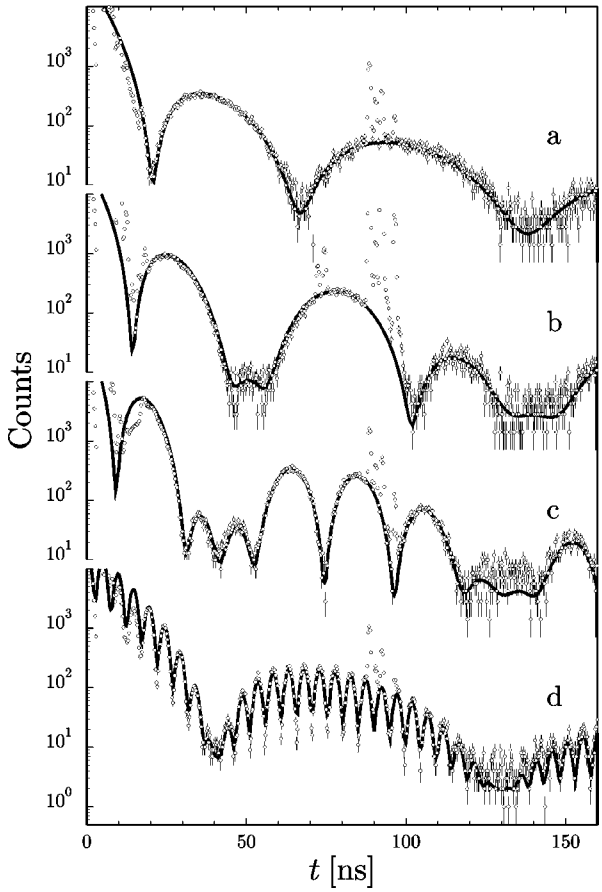

Figure 5. Time evolution of NFS of SR from two ∼7 μm SS foils, where one foil was moved at constant velocities corresponding to Doppler shifts of 0 (a), 20 (b), 40 (c) and 180Γ_0 (d). The solid lines are fits using the NFS theory [11].

regime is already reached at $\Delta E \sim 40\Gamma_0$, where the QB structure is modulated by the DB, as observed, e.g., in figure 5c for the DB minimum at ∼40 ns.

This melting together of QB and DB was also demonstrated in the case of a real quadrupole splitting, where the time evolution of NFS of SR through a single crystal platelet of $^{57}FeBO_3$ of thickness ∼30 μm was studied [20]. Above the Néel temperature this material has a quadrupole splitting of $\sim 4\Gamma_0$. The time evolution of NFS measured at 348.4 K, i.e., slightly above the Néel point, is shown in figure 6 together with the calculated energy dependence of the NFS intensity used. The time spectrum exhibits a slow hybrid beat. The corresponding energy spectrum is particularly remarkable. It gives no indication of the quadrupole splitting, which is completely covered by the overall interference process leading to the pronounced double-hump structure.

Thus when the energy separation of discrete resonances is not large in comparison to the double-hump splittings, QB and DB can no longer be identified. Instead, they

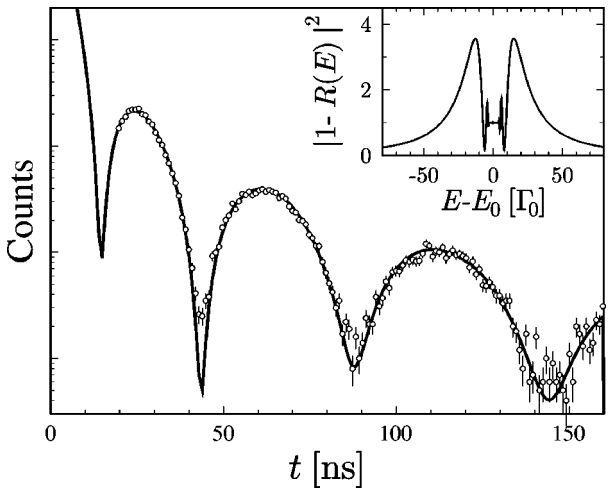

Figure 6. Time evolution and energy distribution of NFS of SR for a 30 μm $^{57}FeBO_3$ single crystal platelet above the Néel temperature. The solid lines are fits using the NFS theory [11].

blend into hybrid forms of beating. A typical example is also shown in figure 1c, where the time spectrum exhibits a dynamical modulation with strongly shifted zeroes as compared to the DB of figure 1a. So already in the case of a simple quadrupole splitting the interference effects involved make the spectra of NFS by optically thick samples rather complex in structure and inaccessible for direct interpretation without computer analysis.

3.2. Fast hybrid beat

The situation becomes even less transparent when NFS by a continuous distribution of resonances is considered. Distributions of hyperfine field parameters are usually directly connected with the nature of the sample under study, as, for example, magnetic field distributions in intermetallic alloys. But they might also be produced by the experimental technique, e.g., by pressure gradients hardly avoidable in high-pressure cells. Because of the importance of these effects, the influence of resonance broadening and of continuous resonance distributions on NFS of SR was recently considered in a comprehensive study [12].

An Invar alloy of composition $Fe_{65}Ni_{35}$, enriched to 95% in ^{57}Fe, was used as sample material. Such alloys are ferromagnetic and considered in Mössbauer spectroscopy as classical, but still disputed [21–23] as examples of predominantly inhomogeneous resonance broadening due to static magnetic hyperfine field distributions. At room temperature they exhibit an asymmetric broadening of several natural linewidths Γ_0 [21]. The time dependence of NFS of SR was studied for Invar foils in the thickness range from ∼1–70 μm.

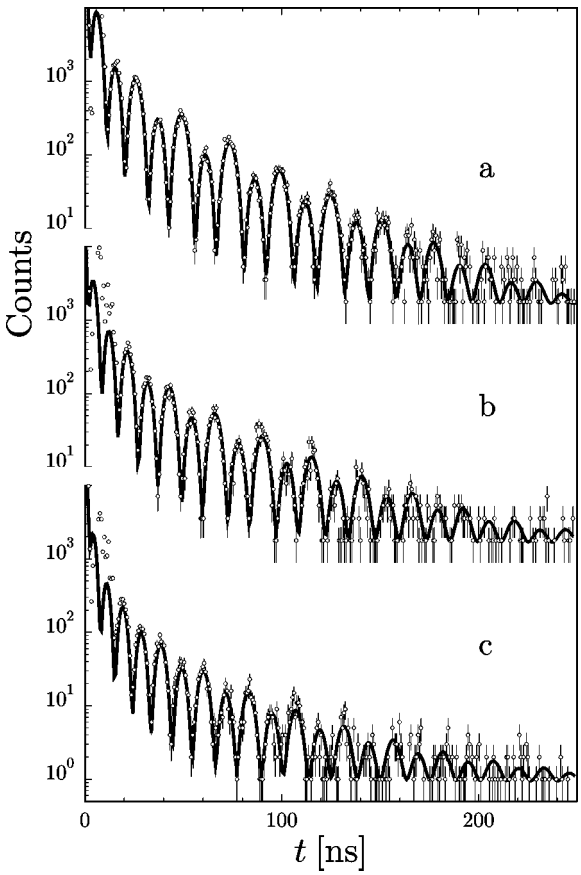

Figure 7. Time evolution of NFS of SR for a 40 μm Invar foil in a vertical magnetic field of ∼0.13 T. Foil mounted perpendicular to the beam (a) and inclined by ∼45° (b) and ∼58° (c), yielding effective thicknesses of 40, 57 and 76 μm, respectively. The solid lines are fits using the NFS theory [11].

Figure 7 shows typical results for a foil of ∼40 μm thickness at different inclinations with respect to the beam, yielding effective foil thicknesses of 40, 57 and 76 μm, respectively. The foil was placed in a vertical magnetic field of ∼0.13 T, so that only the scattering by the $M - m = 0$ hyperfine transitions is observed. As with thinner foils, three unexpected features are noticed:

1. The apparent QB has periods much shorter than expected from the hyperfine splitting in Invar. The period decreases with increasing effective foil thickness.
2. No modulation by a DB can be recognised.
3. The apparent QB shows a perceptible high–low modulation.

Model considerations and fitting results indicate that the absence of the DB modulation might be connected with an asymmetry of the field distribution, which is typical for Invar at room temperature [21]. At low temperatures, by contrast, the field dis-

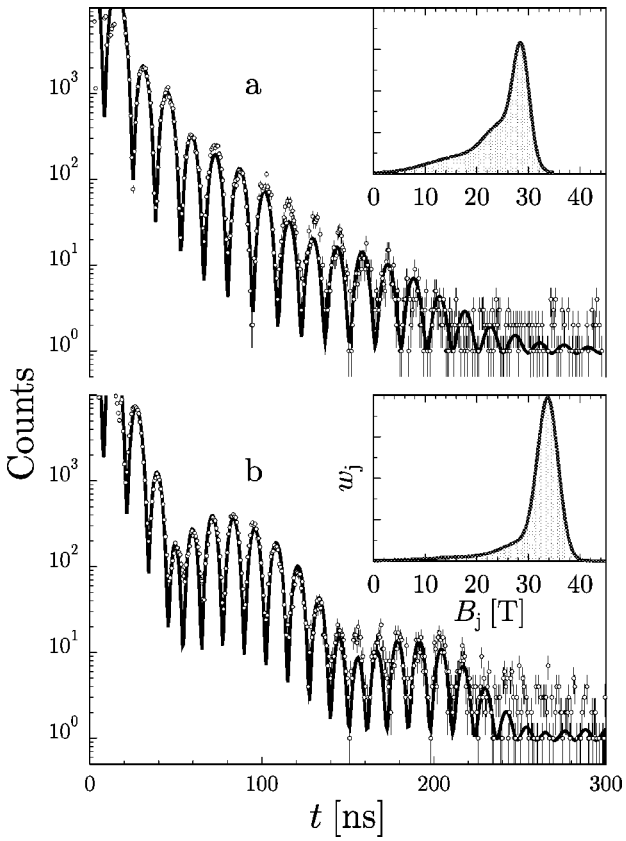

Figure 8. Time evolution of NFS of SR for a 6 μm Invar foil at room temperature in a vertical magnetic field of ∼0.13 T (a) and at 4 K in a vertical magnetic field of 1 T (b). The solid lines are fits using the NFS theory [11]. The insets show the field distributions used for the fit.

tribution is much more symmetrical [21]. In order to check the influence of different resonance shapes, the NFS of a 6 μm Invar foil was compared at room temperature and at 4 K (figure 8). Whereas the time spectrum at room temperature (figure 8a) gives no indication of a DB, the time dependence at 4 K (figure 8b) reveals a DB envelope with rather pronounced minima around 50 and 150 ns. This experiment proves that the absence of a DB at room temperature is connected with the shape of the field distribution rather than with thickness inhomogeneities of the foil or other reasons.

Finally, it was realized that all time dependences could be consistently fitted by assuming an asymmetric resonance broadening caused by asymmetric magnetic field distributions. The effect of resonance broadening on the two double-hump structures and on the corresponding time evolutions of NFS of SR is summarised in figure 9. In figure 9a a definite value was assumed for the magnetic field, as in the case of iron metal, for instance. The resulting double-hump structures are well shaped, and in the time spectrum a fast QB is modulated by a pronounced DB. In figures 9b and 9c sym-

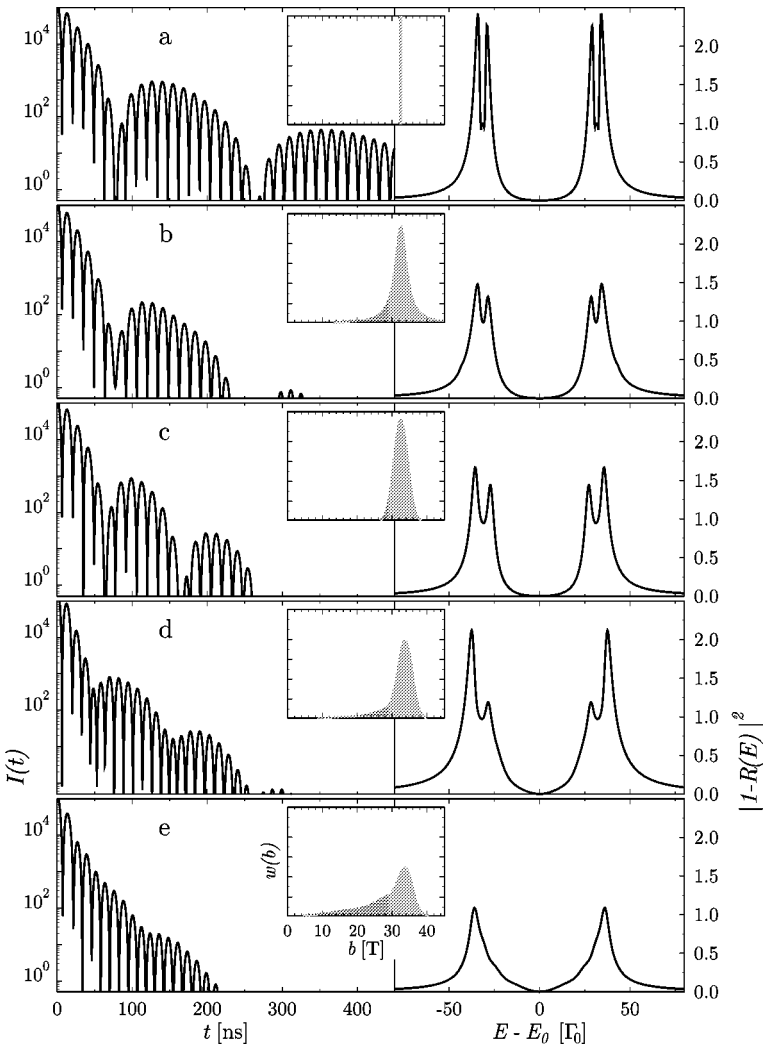

Figure 9. Time evolution of NFS (left), energy dependence of NFS (right) and field profile (center) for different magnetic field distributions: definite value of magnetic field (a), symmetrical distributions of Lorentzian shape (b) and of Gaussian shape (c), slightly asymmetrical distribution corresponding to Invar at 4 K (d) and strongly asymmetrical distribution (e) based on Invar at room temperature.

metrical distributions of Lorentzian and Gaussian shape, respectively, were assumed. The general double-hump character and the resulting strong modulation of the time spectrum by a DB remain essentially unchanged. In particular, the Lorentzian field distribution does not change the positions of the QB and DB minima, as noted previously [24–26]. The essential influence of the Lorentzian inhomogeneous broadening is a faster decay of the NFS signal. In the case of Gaussian broadening, by contrast, the QB modulation remains unchanged, whereas the DB minima are shifted to earlier times [12].

A fundamental change, however, occurs, when an asymmetry is introduced in the field distribution. For asymmetric broadening, with oscillator densities $w(b)$ which decrease more slowly in the region between the resonances than outside them, the inner humps are much more affected by destructive interference than the outer ones (see figure 9d). For a pronounced asymmetry, they can even be completely cancelled (see figure 9e). These hump structures then yield NFS time evolutions with less pronounced or finally completely missing DB modulations (figures 9d and e). Note that the field distribution of figure 9d is actually the one used for the fit of the NFS by the 6 μm Invar foil measured at 4 K (compare figure 8b). The field distribution of figure 9e is the one used for the fit of the NFS of the same foil measured at room temperature (compare figure 8a), however with the internal fields scaled so that the highest one corresponds to the one of figures 9a–d.

Thus, the reason for the vanishing DB modulation at room temperature is the interference of scattering contributions from neighbouring resonances, which leads for an asymmetric oscillator distribution to a strong deformation of the energy dependence of NFS of SR.[1] This already occurs for scattering by optically thin targets [12]. For optically thick targets, such asymmetric distributions can obviously make the inner humps of each pair of humps disappear almost completely, as seen in figure 9e. This gives an explanation for the anomalous features observed for thick Invar foils (compare figure 7): DB and QB cease to exist separately, and instead blend into a new fast hybrid beat. This hybrid beat originates from the interference of the radiation components associated with the two outer humps, with a beat frequency given approximately by $\omega_{\mathrm{Q}} + \omega'_{\mathrm{D}}$ (compare figure 1b, with the two inner humps cancelled). Since ω'_{D} increases with sample thickness, the period of the hybrid beat decreases, as observed in the experiment.

The NFS of SR by another common Invar system, $Fe_{72}Pt_{28}$, is presently under study [28]. This material, however, exhibits only a relatively small and symmetrical field distribution as compared to $Fe_{65}Ni_{35}$ [29]. Correspondingly, the time evolution of NFS still exhibits a DB [28]. In light of this experiment the vanishing of the DB for $Fe_{65}Ni_{35}$ has to be considered as an extreme but not uncommon case.

The fast hybrid beat is typical for large hyperfine splittings for strongly asymmetric magnetic field distributions. Since it has a shorter period than the original QB, it would yield erroneous values for the hyperfine splitting, if it is misinterpreted as a pure QB.

[1] A similar problem is known in X-ray physics, where the peculiar shape of the refractive index near an atomic edge is caused by asymmetric resonance broadening [27]. Near an atomic edge, the atomic oscillator distribution, as obtained by X-ray absorption measurements, is extremely asymmetric, resembling a saw-tooth distribution. For each oscillator of this distribution, the scattering amplitude is negative above and positive below resonance. Within the distribution, the scattering amplitudes above the individual resonances are almost cancelled by corresponding amplitudes of opposite sign belonging to neighbouring resonances of slightly higher energy. As a result, only a small positive amplitude below the atomic edge remains. The essential point here is that the real part of resonant scattering, which changes sign at resonance, is extremely sensitive to the particular distribution of oscillators.

4. Summary

In NFS of SR by materials that exhibit several resonances, intra-resonance and inter-resonance interference appear in parallel, and in general cause complicated hybrid forms of beating. Three types of interference patterns can be distinguished.

When the separation of the resonances is large in comparison with the extension of the double-hump structures, the single-resonance approximation can be used. In this case the modulation of the time evolution can still be analysed in terms of a combination of DB and QB. A good example of this type of interference pattern is the NFS by the $M - m = \pm 1$ hyperfine transitions in Fe metal.

For near neighbouring resonances, however, inter-resonance and intra-resonance interference are strongly mixed and can no longer be identified. A small quadrupole splitting, for instance, leads to a slow hybrid beat, which can be recognised by a shift of the zeroes of the dynamical modulation.

For a continuous distribution of resonances, the result of the interference depends strongly on its shape. A Lorentzian distribution, for instance, leaves DB and QB unchanged, and only causes a faster decay of the signal. By contrast, strongly asymmetric distributions, which occur, for instance, in Invar alloys, can make DB and QB blend into a fast hybrid beat with thickness dependent period and distribution dependent modulation.

Acknowledgements

This work has been funded by the Bundesministerium für Bildung, Wissenschaft, Forschung und Technologie under contracts 05 643WOA/SK8WOA and 05 643GUA1. The authors would like to thank G.V. Smirnov, W. Potzel, P. Schindelmann and H.D. Rüter for fruitful discussions.

References

[1] E. Gerdau, R. Rüffer, H. Winkler, W. Tolksdorf, C.P. Klages and J.P. Hannon, Phys. Rev. Lett. 54 (1985) 835.
[2] E. Gerdau and U. van Bürck, in: *Resonant Anomalous X-ray Scattering, Theory and Applications*, eds. G. Materlik, C.J. Sparks and K. Fischer (North-Holland, Amsterdam, 1994) p. 589.
[3] G.V. Smirnov, Hyp. Interact. 97/98 (1996) 551; in: *X-ray and Inner-Shell Processes*, eds. R.L. Johnson, H. Schmidt-Böcking and B.F. Sonntag, AIP Conference Proceedings 389, Woodbury, New York (1997) p. 323.
[4] J.B. Hastings, D.P. Siddons, U. van Bürck, R. Hollatz and U. Bergmann, Phys. Rev. Lett. 66 (1991) 770.
[5] G.T. Trammell and J.P. Hannon, Phys. Rev. B 18 (1978) 165; Erratum in Phys. Rev. B 19 (1979) 3835.
[6] E. Gerdau, R. Rüffer, R. Hollatz and J.P. Hannon, Phys. Rev. Lett. 57 (1986) 1141.
[7] F.J. Lynch, R.E. Holland and M. Hamermesh, Phys. Rev. 120 (1960) 513.
[8] Yu. Kagan, A.M. Afanas'ev and V.G. Kohn, J. Phys. C: Solid State Phys. 12 (1979) 615.

[9] Yu.V. Shvyd'ko, S.L. Popov and G.V. Smirnov, Pis'ma. Zh. Eksper. Teoret. Fiz. 53 (1991) 217 (JETP Lett. 53 (1991) 231); J. Phys. C: Condens. Matter 5 (1993) 1557; Erratum in ibid. 5 (1993) 7047.
[10] U. van Bürck, D.P. Siddons, J.B. Hastings, U. Bergmann and R. Hollatz, Phys. Rev. B 46 (1992) 6207.
[11] Yu.V. Shvyd'ko, Phys. Rev. B 59 (1999) 9132; also this issue, section III-1.3.
[12] Yu.V. Shvyd'ko, U. van Bürck, W. Potzel, P. Schindelmann, E. Gerdau, O. Leupold, J. Metge, H.D. Rüter and G.V. Smirnov, Phys. Rev. B 57 (1998) 3552.
[13] U. van Bürck, this issue, section IV-2.1.
[14] S. Kikuta, in: *Resonant Anomalous X-ray Scattering, Theory and Applications*, eds. G. Materlik, C.J. Sparks and K. Fischer (North-Holland, Amsterdam, 1994) p. 635.
[15] A.I. Chumakov, G.V. Smirnov, M.V. Zelepukhin, U. van Bürck, E. Gerdau, R. Rüffer and H.D. Rüter, Europhys. Lett. 17 (1992) 269.
[16] U. van Bürck, W. Potzel, P. Schindelmann, G.V. Smirnov, S.L. Popov, E. Gerdau, O. Leupold, Yu.V. Shvyd'ko and H.D. Rüter, HASYLAB Ann. Report (1996) 884.
[17] Yu.V. Shvyd'ko and E. Gerdau, this issue, section IV-3.4.
[18] S.L. Popov, Yu.V. Shvyd'ko, J. Jäschke, U. van Bürck, W. Potzel, P. Schindelmann, E. Gerdau, O. Leupold and H.D. Rüter, unpublished.
[19] U. van Bürck, W. Potzel, P. Schindelmann, Yu.V. Shvyd'ko, E. Gerdau, O. Leupold and H.D. Rüter, submitted to Phys. Rev. A.
[20] Yu.V. Shvyd'ko, unpublished.
[21] J.Y. Ping, D.G. Rancourt and R.A. Dunlap, J. Magn. Magn. Mater. 103 (1992) 285.
[22] E.Yu. Tsymbal, A.M. Afanas'ev, M. Fricke and J. Hesse, Hyp. Interact. 93 (1994) 1543.
[23] M. Dubé, P.R.L. Heron and D.G. Rancourt, J. Magn. Magn. Mater. 147 (1995) 122; M.-Z. Dang, M. Dubé and D.G. Rancourt, ibid., 133.
[24] E. Ikonen, P. Helistö, T. Katila and K. Riski, Phys. Rev. A 32 (1985) 2298.
[25] Yu.V. Shvyd'ko and G.V. Smirnov, Nucl. Instrum. Methods in Phys. Res. B 51 (1990) 452.
[26] G.V. Smirnov and V.G. Kohn, Phys. Rev. B 52 (1995) 3356.
[27] R.W. James, *The Optical Principles of the Diffraction of X-rays* (G. Bell and Sons, London, 1958) chapter IV.1.(k).
[28] N. Wiele, H. Franz, W. Petry and O. Leupold, HASYLAB Ann. Report (1997) 935.
[29] U. Gonser, S. Nasu and W. Kappes, J. Magn. Magn. Mater. 10 (1979) 244.